Linking Pre- and Perinatal Risk Factors to a Multivariate Fusion of Child Cortical Structure

Linn R. S. Lindseth[a,b], Dani Beck[a,b], Lars T. Westlye[c,d,e], Christian K. Tamnes[a,b], Linn B. Norbom[a]

[a] PROMENTA Research Center, Department of Psychology, University of Oslo, Oslo, Norway

[b] Division of Mental Health and Substance Abuse, Diakonhjemmet Hospital, Oslo, Norway

[c] Department of Psychology, University of Oslo, Oslo, Norway

[d] Center for Precision Psychiatry, Division of Mental Health and Addiction, Oslo University Hospital, Oslo, Norway

[e] KG Jebsen Centre for Neurodevelopmental Disorders, University of Oslo, Oslo, Norway

*Linn R. S. Lindseth

Email: l.r.s.lindseth@psykologi.uio.no

Author Contributions: LRSL, CKT, and LBN designed the study. LRSL and LBN did the data analysis. LRSL, CKT, and LBN interpreted the data and drafted the manuscript. All authors critically revised and approved the manuscript.

Competing Interest Statement: The authors declare no competing interests.

Keywords: Cortical morphology; MRI; Neurodevelopment; Prenatal; Perinatal

This PDF file includes:

Main Text
References
Figures 1 to 3
Tables 1 to 2

Abstract

Pre- and perinatal factors such as maternal pregnancy and child birth complications affect child brain development, emphasizing the importance of early life exposures. While most previous studies have focused on a few variables in isolation, here, we investigated associations between a broad range of pregnancy- and birth-related variables and multivariate cortical brain MRI features. Our sample consisted of 8,396 children aged 8.9 to 11.1 years from the ABCD Study. Through multiple correspondence analysis and factor analysis of mixed data, we distilled numerous pre- and perinatal variables into four overarching dimensions; maternal pregnancy complications, maternal substance use, compromised fetal growth, and newborn birth complications. Vertex-wise measures of cortical thickness, surface area, and curvature were fused using linked independent component analysis. Linear mixed effects models showed that maternal pregnancy complications and compromised fetal growth, including low birth weight, being born preterm, or as a twin, were associated with smaller global surface area. Additionally, compromised fetal growth was associated with two regional patterns reflecting a complex combination of 1) smaller occipital, inferior frontal and insular cortex, larger fronto-temporal cortex, thinner pre- and post-central cortex, and thicker inferior frontal and insular cortex, and 2) smaller and thicker occipital and temporal lobe cortex, and larger and thinner insular cortex. In contrast, maternal substance use and newborn birth complications showed no associations with child cortical structure. By employing a multifactorial and multivariate morphometric fusion approach, we connected complications during pregnancy and fetal growth to global surface area and specific regional signatures across child cortical MRI features.

Significance Statement

Early life stages, including the prenatal and perinatal periods, are critically important for a wide range of real-life outcomes. In this study, we linked maternal complications during pregnancy and compromised fetal growth to both globally reduced cortical surface area and complex cortical structural patterns later in late childhood. Our findings underscore the importance of providing support to mothers and children during these crucial phases, helping to ensure optimal conditions for healthy child development.

Introduction

Decades of research document that the period from conception to birth is crucial for subsequent development (1, 2). Adverse events and exposures during this time have been linked to a variety of negative outcomes, including lower general cognitive ability (3–6), behavioral problems (6–10), and neurodevelopmental conditions (11, 12).

During both the prenatal phase, i.e. the pregnancy period, and the perinatal phase, the time closely surrounding birth, the cerebral cortex undergoes rapid maturation (13), which mirrors cognitive development (14). The cortical plate begins forming around 7 weeks post-conception (15, 16), and by 20 weeks of gestation it can be observed as a smooth surface in fetal magnetic resonance imaging (MRI) (17). The greatest increase in cortical thickness (CT) occurs mid-gestation, reaching about 80% of its maximum size by birth, while surface area (SA) expands from mid-gestation, reaching approximately 25% of its maximum size at birth (13). Most of the cortical folding occurs during the final trimester of pregnancy (17, 18).

Postnatal development of the cerebral cortex is characterized by a continued thickening for the first two years of life (13, 19, 20), followed by a gradual thinning throughout childhood and adolescence (13, 21, 22). SA increases rapidly the first two years of life (13, 23) and continues to expand at a slower pace until middle childhood (13), followed by a subtle decrease through adolescence (13, 21, 22). Cortical folding increases during the first years of life (24), before slowly decreasing (21). Cortical development also exhibits both individual (25, 26) and sex (21) differences, and studies have shown that cortical morphology is highly heritable (27). Despite this strong genetic influence, environmental factors and experiences can fundamentally shape cortical structure.

A wide range of early-life environmental risk factors have been linked to variations in child cortical morphology in childhood and adolescence. Maternal pregnancy-related complications such as pre-eclampsia and high blood-pressure have been associated with both increased (9, 28) and decreased (3) CT, as well as smaller SA (6, 28). Prenatal exposure to substances has been associated with bot increased (10, 29–32) and decreased (7, 10, 31) CT, and both larger (8) and smaller (29, 33, 34) SA. Further, a range of perinatal variables, including caesarian delivery, being born before due date, and lower birth weight, have been related to increased CT (28, 35–39), though lower birth weight has also been associated with decreased CT (5, 37–39). Several perinatal variables have also been associated with smaller SA (5, 28, 35–40). Although research on cortical folding is more limited, studies suggest that various pre- and perinatal variables are associated with altered sulcal patterns (10, 28) and gyrification (36).

Our current understanding of the complex relationships between pre- and perinatal variables and future cortical structure is limited by that most previous studies have focused on one or a few variables and one or a few brain metrics in isolation. In contrast, investigating a broad set of pre- and perinatal variables could provide insight into potentially overlapping effects of diverse pregnancy- and birth-related risk factors. Further, it is likely that multiple biological processes, here captured by partly separate cortical metrics, are both uniquely and collectively influenced by pre- and perinatal factors. Indeed, a recent study that assessed a wide range of environmental variables along with multiple neuroimaging metrics revealed complex relationships between pre- and perinatal factors and child brain structure (28).

In a sample of 8,396 participants aged 8.9 to 11.1 years (Mean = 9.92, SD = 0.63, 47.9% female) from the Adolescent Brain Cognitive Development (ABCD) Study (https://abcdstudy.org/), we tested the associations between a broad set of pre- and perinatal risk factors and child cortical structure, assessed through fusion of CT, SA, and curvature. Pre- and perinatal variables included maternal somatic health in pregnancy, substance use, and birth complications. We hypothesized that exposures to pre- and perinatal risk factors would be linked to higher CT (9, 28–32) and lower SA (6, 28, 33–35, 37–41) of the child, grossly reflecting a less mature brain.

Additionally, we expected pre- and perinatal risk to be associated with regionally altered cortical curvature (10, 28, 36).

Results

Pre- and Perinatal Dimensions

Using the ABCD Developmental History Questionnaire (42), we identified 23 prenatal and 12 perinatal variables, which were reduced to overarching dimensions using Factor Analysis of Mixed Data (FAMD) and Multiple Correspondence Analysis (MCA). For further analyses, we selected the first two dimensions from both reduction methods, which explained 9.2% and 7.1% of the total prenatal variance, and 22.8% and 14.4% of the total perinatal variance, respectively (SI Appendix Fig. S1). We labeled the first prenatal dimension “Maternal Pregnancy Complications” as it comprised variables relating to maternal somatic health during pregnancy, including occurrence of rubella, proteinuria, high blood-pressure, and (pre-)eclampsia. We labeled the second prenatal dimension “Maternal Substance Use”, which included variables related to use of tobacco, marijuana, and alcohol, in addition to other substances. We named the first perinatal dimension “Compromised Fetal Growth” as the most contributing variables were related to compromised growth of the child, such as weeks born before due date, birth weight, and twin pregnancy. The second perinatal dimension, “Newborn Birth Complications”, was characterized by variables such as the child appearing blue in color, not breathing, or having a slow heartbeat. The most contributing variables and their explained variance in the given dimensions are shown in Fig. 1, while density plots for the selected dimensions are shown in SI Appendix Fig. S2. Further details on the results of the reduction analysis are presented in the “Methods” section of the SI Appendix. Loadings of the contributing variables in the dimensional space are illustrated in in SI Appendix Fig. S3.

Cortical Decomposition

Final decomposition of vertex-wise surface maps of CT, SA, and curvature yielded 39 independent cortical components (CC) (Fig. 2). In general, SA contributed most to the components overall, followed by CT, while curvature only had minor contributions. The components captured both unique and multivariate patterns, and the respective weighting and explained variance are presented in SI Appendix Tab. S1. CC1 accounted for 29.30% of the total variance in the imaging data, while the remaining CCs explained between 7.26% and 0.99%.

Associations Between Pre- and Perinatal Dimensions and Cortical Structure

Linear mixed effects modelling revealed a significant negative association between Maternal Pregnancy Complications and CC1 ($t = -4.50$, Cohen´s $D = -0.10$, $p_{adjusted} < 0.001$) (Tab. 1 and Fig. 3). CC1 was dominated by global SA, indicating that mothers who experienced somatic health complications during pregnancy had children with smaller global SA at approximately age 10 compared to mothers with fewer such complications.

Further, the results revealed significant associations between Compromised Fetal Growth and CC1, CC6, and CC8 (Tab. 2 and Fig. 3). Compromised Fetal Growth was negatively associated with CC1 ($t = -3.93$, Cohen´s $D = -0.09$, $p_{adjusted} = 0.003$), indicating that children experiencing compromised fetal growth had smaller global SA at around 10 years of age. Compromised Fetal Growth also showed a negative association with C6 ($t = -3.24$, Cohen´s $D = -0.08$, $p_{adjusted} = 0.044$. CC6 reflected a multivariate pattern including SA, CT, and to a less degree curvature. These results indicate that in addition to the overall association between Compromised Fetal Growth and globally smaller SA, children with compromised fetal growth had regionally smaller occipital, inferior frontal and insular area, as well as a larger regional fronto-temporal area, coupled with thinner pre- and post-central cortices and thicker inferior frontal and insula cortices. Finally, Compromised Fetal Growth showed a positive association with CC8 ($t = 4.15$, Cohen´s $D = 0.10$, $p_{adjusted} = 0.001$), which captured SA, CT, and to a less degree curvature. This indicates that in addition to the associations reported, children who experienced compromised fetal growth

appeared to have smaller and thicker occipital cortex and larger and thinner insular cortex at about 10 years of age.

There were no significant associations between either Maternal Substance Use (Tab. 1) or Newborn Birth Complications (Tab. 2) and any of the CCs.

Discussion

The developing fetus is highly sensitive to its intrauterine environment and events occurring around the time of birth. In this study, we employed a multifactorial and multivariate fusion imaging approach to investigate how a diverse range of pre-and perinatal risk factors are associated with variation in cortical morphometry in late childhood. Our findings showed that children whose mothers experienced somatic health complications during pregnancy, as well as children with compromised fetal growth, exhibited smaller global SA. Additionally, children with compromised fetal growth demonstrated distinct regional cortical patterns.

Our findings linking maternal pregnancy complication to smaller global SA of the child align with previous ABCD Study findings investigating either a single or a few prenatal variables and regional cortical measures (3, 6, 9), as well as a previous multifactor multivariate fusion study (28). Smaller human imaging studies and animal studies have also linked maternal pregnancy complications to altered brain structure in the offspring (9, 43–46). Our results also support prior research linking compromised fetal growth with reduced global or widespread SA in children (5, 28, 35–41). A longitudinal study comparing term-born and preterm-born children showed that the difference in SA is mostly established at birth, and that most cortical regions displayed similar SA developmental trajectories over time (39). Further, our multivariate fusion approach of cortical data allowed us to move beyond well-established associations between pre- and perinatal risk factors and unique SA effects, revealing additional regional patterns across different morphometrics.

Our findings align with the previous studies that found no associations between fetal growth and global CT (5, 37, 41) but instead with regional CT variations (36–38). Our first shared multivariate pattern (CC6) is consistent with previous studies indicating thicker inferior frontal (39), thinner temporal (36, 39), thinner pre-and post-central (37), and a thicker medial inferior frontal (38) cortex. Our second shared pattern (CC() showing thicker occipital cortex also support previous findings (37, 39). However, other studies report more widespread, different, or contradictory patterns of regional CT (36–39).

Overall, our results indicate that maternal pregnancy complications and compromised fetal growth have global homogenous effects on child SA and regional heterogenous effects on child CT (39). Premature birth will cause the fetus to miss the later part of pregnancy, a critical period for in-utero SA expansion (13, 36). In contrast, the peak growth of CT occurs mid-gestation, which could explain some of the divergent effects observed on CT compared to SA.

Our analysis revealed no significant associations between maternal substance use and later child cortical structure, which contrasts previous studies (7, 8, 10, 29–34). This discrepancy may be due to several factors, including relatively low variance in several of the maternal substance use variables in the ABCD sample, reliance on self-reported data that may have led to underreporting, and that we were unable to account for dose, frequency, and timing of substance use. However, potential associations may have gone undetected, as we did not explore indirect mediation effects. Previous research suggests that maternal substance use can influence fetal size (47, 48), which may subsequently impact the child's cortex—an association that we observed. We also found no significant associations between newborn birth complications and cortical structure. However, the aspect of needing oxygen at birth was captured in the compromised fetal growth dimension, associated with patterns of reduced SA in line with previous studies (41). Finally,

multifactorial data-driven reduction methods could mask potential specific effects, but this is speculative.

Contrary to previous studies on cortical folding (6, 28, 36), we found minimal relations between pre- and perinatal risk factors on child cortical curvature. This discrepancy is likely due to our cortical components having limited contributions from curvature, thereby restricting our ability to thoroughly test these association from the outset. Moreover, differences in the measures of cortical folding and other methodological aspects could also account for the discrepant findings.

Although caution is warranted when interpreting neurobiological maturity based on cross-sectional findings, cortical differences in late childhood associated with pre- and perinatal factors have been suggested to reflect brain maturity (3–6, 9, 37, 39). Smaller global SA and differences in parahippocampal and frontal cortex have been associated with lower general cognitive ability in children born with very low birth weight (37). Recent studies have also found a relationship between being born pre-term and CT differences in language areas (49) and in inferior frontal and medial parietal regions as well as impaired language and memory function (39).

One potential mechanism underlying the relationship between maternal pregnancy complications, compromised fetal growth, and child cortical structure is fetal exposure to maternal stress during pregnancy (50, 51). Proxies for maternal stress such as prenatal depression have been associated with pregnancy complications (52, 53), fetal growth (54, 55), and child cortical structure (56, 57). Fetal exposure to maternal stress may impair the barrier of the placenta by affecting an enzyme (11beta-hydroxysteroid dehydrogenase type 2 (11β-HSD2)) involved in stress regulation, allowing for more stress hormones to reach the fetus (58, 59). Indeed, reduced activity of 11β-HSD2 has been associated with incidences of both pre- and perinatal risk factors (60–62). A possible mechanism underlying our findings related to perinatal risk factors and child cortical structure is hypoxia, i.e. the lack of sufficient oxygen to the baby's brain during delivery (63), indicated by the variable oxygen treatment in the present study. Hypoxia is associated with neural harm (41, 64), changes in number of neurons (37, 65), and accelerated neuronal maturation (66). Regional differences in cortical associations with hypoxia may be explained by the location of different cerebral vessels (41, 64). More generally, associations between pre-and perinatal factors and cortical structure in the child could be explained by shared genetic susceptibility between pre- and perinatal factors and child cortical morphometry (36, 67, 68) and epigenetics effects such as DNA methylation (35).

The current study has several limitations. First, pre- and perinatal data were obtained from retrospective self-reporting. Second, our observational study does not allow for causal inferences. Third, while considering a wide array of pre- and perinatal risk factors offers a comprehensive perspective, it comes at the expense of not addressing specific details such as the timing and dose of substance use, number and severity of pre- and perinatal complications (41, 69), and the timing of prenatal events (70). Finally, the present sample is not ethnically representative, with nearly 80% of participants identifying as white. The ABCD Study in general is less representative for rural populations (71), as well as with respect to family income and education (72).

Our study revealed that maternal somatic health during pregnancy and compromised fetal growth were associated with unique global surface area signatures as well as shared regional patterns across cortical morphometry later in the child's life. While specific neurobiological mechanisms remain to be explored, our findings highlight the importance of supporting mothers and their unborn babies during critical periods to foster optimal child development.

Materials and Methods

Sample

The data was drawn from the ABCD Study, a dataset comprising nearly 12.000 children aged 9-11 years, along with their parents. This ongoing longitudinal study tracks brain development and child health across the US, with data collected from 21 research centers located across the country (https://abcdstudy.org/). The current study used data from the baseline assessment, release 4.0. Of the 11.876 participants, 9758 had pre-processed, quality controlled vertex-wise imaging data (73). From these, 1327 children were excluded due to their ABCD Developmental History Questionnaire (42) being completed by their non-biological mother. An additional 35 participants were excluded due to having more than 15% missing responses for the pre- and perinatal variables of interest. This yielded a final sample of 8396 participants aged 8.9 – 11.1 years (mean = 9.9, SD = 0.6), including 582 twins (291 pairs) and 2558 siblings. Sample demographics are presented in SI Appendix section "Methods", SI Appendix Fig. S4 and SI Appendix Tab. S2.

Assessment of Pre- and Perinatal Factors

Pre- and perinatal variables were collected through retrospective reporting from the biological mother using the ABCD Developmental History Questionnaire (42). From this questionnaire, 23 prenatal variables and 12 perinatal variables were identified. An overview of included variables is provided in SI Appendix Tab. S3, with further details about questions provided in SI Appendix Table S4 and recoding of variables in SI Appendix section "Methods". A correlation matrix for the variables is shown in SI Appendix Fig. S5. As expected, several of the variables showed near-zero variance as identified using the "nearZeroVar" function from the caret-package (version 6.0-92) in R, version 4.2.1 (https://www.r-project.org/). (SI Appendix Tab. S5). Despite potentially offering less information about the dependent variable and concerns of overfitting, we decided to keep all selected variables as rare extreme factors (e.g. maternal use of oxycontin and maternal infection of rubella during pregnancy) could be highly influential on cortical structure, and as they could be aggregated into overarching factors, thereby amplifying overall variance. Results from analyses excluding variables with near-zero variance at a rate of >0.99 for the most common to the second most common response (SI Appendix Tab. S5) yielded similar results (SI Appendix Fig. S6-S8 and SI Appendix Tab. S6-S7). Missing pre- and perinatal values were imputed using the mice-package (version 3.14.0) in R. Continuous variables, birth weight and weeks born before due date, were z-standardized.

We used the "MCA" and "FAMD" functions from the FactoMineR package (version 2.4) in R to reduce and extract underlying factors from the pre- and perinatal variables, which were split accordingly. MCA was applied to the binary prenatal variables, while FAMD handled the mixed binary and continuous perinatal variables. This reduction yielded several dimensions, and we chose two for each set of variables for further analyses, which were z-standardized. Results from reduction analyses excluding missing data instead of imputing were consistent (SI Appendix Fig. S9-S10).

MRI Acquisition, Preprocessing, and Quality Control

The MRI data was acquired on 29 different 3T scanners from Siemens Prisma, Philips, and General Electric (GE) 750 (74). T1-weighted images were obtained through an inversion-prepared RF-spoiled gradient echo scan, featuring 1-millimeter isotropic voxel resolution, and was consistently performed as the second sequence. An adult-sized coil was used. Further details regarding the MRI acquisition, including parameters for the scans, are provided elsewhere (74). The T1-weighted images underwent an initial quality control by the ABCD-team, checking for quality issues such as incorrect acquisition parameters, imaging artifacts, or corrupted data files, using both automated and manual methods (75). 367 participants were excluded due to not passing this binary include/exclude quality control (73, 75).

We processed the T1-weighted images using FreeSurfer 7.1 (https://surfer.nmr.mgh.harvard.edu/) (76, 77). The present study used vertex-wise calculations of cortical morphology (76), specifically CT, SA, and curvature (see SI Appendix section "Methods"

for details). 104 participants were excluded due to missing surface data (73). FreeSurfer also calculates the quality metric Euler number, which reflects the total amount of holes in the initial surface (78). 64 participants were excluded due to having surface holes =< 200 (73). CT, SA, and curvature surface maps were mapped to FreeSurfer´s standard space *fsaverage* and smoothed with a Gaussian kernel of 15mm full width at half maximum (FWHM) to increase signal and contrast. Finally, neuroComBat in R was used to harmonize the data across the 29 scanners to adjust for systematic and unwanted scanner related variance (79). Age, sex, p-factor, parental income, and parental education were included as covariates in the harmonization procedure (73).

Multivariate Fusion of Cortical Metrics

CT, SA, and curvature were fused using FMRIB's Linked Independent Component Analysis (FLICA) (80). FLICA can reduce and fuse large amounts of data into independent components across different metrics, even if the input has different smoothness and signal- and contrast to noise. FLICA finds shared patterns across metrics but can also capture univariate patterns when present (80, 81). In the current study, we employed FLICA with 1000 iterations and explored model orders ranging from 20 to 50 components. Logarithmic transformation was applied exclusively to the SA data.

We chose a model order of 40 cortical components based on qualitative assessments of distinct patterns, as well as the cophenetic correlation coefficient (SI Appendix Fig. S11). A cophenetic correlation coefficient represents how well the original data structure is being captured at the chosen number of components (73). One component was driven by a one single subject (SI Appendix Fig. S12) and was excluded from further analyses, yielding a final number of 39 cortical components.

Statistical Analysis

All statistical analyses were conducted in R. Associations between the pre- and perinatal dimensions and each of the cortical components were tested by linear mixed effects modelling using the “lmer” function from the lme4-package (version 1.1-29). The “lme-dscore” function from the EMAtools-package (version 0.1.4) was used to calculate Cohen´s D. The 39 cortical components were dependent variables, while the four pre-and perinatal dimensions were independent variables in separate models, resulting in a total of 156 models. In all models, age and sex were added as fixed effects, while family status (coded with a unique value for each family) and zygosity (with each monozygotic twin-pair receiving an identical value) was modelled as random effects to address dependency in the data. All continuous variables not yet z-standardized were then z-standardized. Due to multiple comparisons, p-values were adjusted by family-wise error rate using the “p.adjust” function and “hochberg”’ method in R, separately for each pre- and perinatal dimension. Significance threshold was set to corrected <0.05. All statistical code used in R is available online (https://osf.io/xeufj/).

Ethical Considerations

Each ABCD site is responsible for following ethical guidelines related to implementation of the study, and each site has developed site-specific standard procedures for the implementation of these guidelines (82, 83). All procedures were approved by a central Institutional Review Board (IRB) at the University of California, San Diego (82), while an External Advisory Board is monitoring ethical issues (84). Parental and child informed consent have been obtained for all participants (82, 83). The present study was conducted in line with the Declaration of Helsinki and was approved by the Regional Committee for Medical and Health Research Ethics (REK 2019/943).

Acknowledgments

Data used in the preparation of this article were obtained from the ABCD Study (https://abcdstudy.org), held in the NIMH Data Archive. This is a multisite, longitudinal study designed to recruit more than 10,000 children aged 9-10 and follow them over 10 years into early

adulthood. The ABCD Study® is supported by the National Institutes of Health and additional federal partners under award numbers U01DA041048, U01DA050989, U01DA051016, U01DA041022, U01DA051018, U01DA051037, U01DA050987, U01DA041174, U01DA041106, U01DA041117, U01DA041028, U01DA041134, U01DA050988, U01DA051039, U01DA041156, U01DA041025, U01DA041120, U01DA051038, U01DA041148, U01DA041093, U01DA041089, U24DA041123, U24DA041147. A full list of supporters is available at https://abcdstudy.org/federal-partners.html. A listing of participating sites and a complete listing of the study investigators can be found at https://abcdstudy.org/consortium_members/. ABCD consortium investigators designed and implemented the study and/or provided data but did not necessarily participate in the analysis or writing of this report. This manuscript reflects the views of the authors and may not reflect the opinions or views of the NIH or ABCD consortium investigators. This work was funded by the Research Council of Norway (#288083, #300767, #323951), the South-Eastern Norway Regional Health Authority (#2021070, #2023012, #500189), and the European Research Council under the European Union's Horizon 2020 research and Innovation program (ERC StG Grant No. 802998).

References

1. D. Almond, J. Currie, Killing Me Softly: The Fetal Origins Hypothesis. *J Econ Perspect* **25**, 153–172 (2011).
2. D. J. P. Barker, Fetal origins of coronary heart disease. *BMJ* **311**, 171–174 (1995).
3. S. Ahmed, M. Á. Cano, M. Sánchez, N. Hu, G. Ibañez, Effect of exposure to maternal diabetes during pregnancy on offspring's brain cortical thickness and neurocognitive functioning. *Child Neuropsychology* **29**, 588–606 (2023).
4. Q. Ma, *et al.*, Lower gestational age is associated with lower cortical volume and cognitive and educational performance in adolescence. *BMC Med* **20**, 424 (2022).
5. A. Raznahan, D. Greenstein, N. R. Lee, L. S. Clasen, J. N. Giedd, Prenatal growth in humans and postnatal brain maturation into late adolescence. *Proc Natl Acad Sci U S A* **109**, 11366–11371 (2012).
6. H. Wang, *et al.*, Severe nausea and vomiting in pregnancy: psychiatric and cognitive problems and brain structure in children. *BMC Medicine* **18**, 228 (2020).
7. H. El Marroun, *et al.*, Prenatal Tobacco Exposure and Brain Morphology: A Prospective Study in Young Children. *Neuropsychopharmacol* **39**, 792–800 (2014).
8. B. Lees, *et al.*, Association of Prenatal Alcohol Exposure With Psychological, Behavioral, and Neurodevelopmental Outcomes in Children From the Adolescent Brain Cognitive Development Study. *AJP* **177**, 1060–1072 (2020).
9. Q. Ma, *et al.*, Association of maternal hypertension during pregnancy with brain structure and behavioral problems in early adolescence. *Eur Child Adolesc Psychiatry* **33**, 2173–2187 (2024).
10. R. Zhang, P. Manza, N. D. Volkow, Prenatal caffeine exposure: association with neurodevelopmental outcomes in 9- to 11-year-old children. *J Child Psychol Psychiatry* **63**, 563–578 (2022).
11. R. H. Bitsko, *et al.*, A Systematic Review and Meta-analysis of Prenatal, Birth, and Postnatal Factors Associated with Attention-Deficit/Hyperactivity Disorder in Children. *Prev Sci* **25**, 203–224 (2024).
12. T. Carlsson, F. Molander, M. J. Taylor, U. Jonsson, S. Bölte, Early environmental risk factors for neurodevelopmental disorders – a systematic review of twin and sibling studies. *Development and Psychopathology* **33**, 1448–1495 (2021).
13. R. A. I. Bethlehem, *et al.*, Brain charts for the human lifespan. *Nature* **604**, 525–533 (2022).
14. J. Dubois, *et al.*, Primary cortical folding in the human newborn: an early marker of later functional development. *Brain* **131**, 2028–2041 (2008).
15. I. Bystron, C. Blakemore, P. Rakic, Development of the human cerebral cortex: Boulder Committee revisited. *Nat Rev Neurosci* **9**, 110–122 (2008).
16. R. L. Sidman, P. Rakic, Neuronal migration, with special reference to developing human brain: a review. *Brain Res.* **62**, 1–35 (1973).
17. C. Fogliarini, *et al.*, Assessment of cortical maturation with prenatal MRI. Part I: normal cortical maturation. *Eur Radiol.* **15**, 1671–1685 (2005).
18. E. Armstrong, A. Schleicher, H. Omran, M. Curtis, K. Zilles, The Ontogeny of Human Gyrification. *Cereb Cortex* **5**, 56–63 (1995).
19. G. Li, W. Lin, J. H. Gilmore, D. Shen, Spatial Patterns, Longitudinal Development, and Hemispheric Asymmetries of Cortical Thickness in Infants from Birth to 2 Years of Age. *J. Neurosci.* **35**, 9150–9162 (2015).
20. A. E. Lyall, *et al.*, Dynamic Development of Regional Cortical Thickness and Surface Area in Early Childhood. *Cereb Cortex* **25**, 2204–2212 (2015).
21. A. Raznahan, *et al.*, How Does Your Cortex Grow? *J Neurosci* **31**, 7174–7177 (2011).
22. C. K. Tamnes, *et al.*, Development of the Cerebral Cortex across Adolescence: A Multisample Study of Inter-Related Longitudinal Changes in Cortical Volume, Surface Area, and Thickness. *J Neurosci* **37**, 3402–3412 (2017).
23. G. Li, *et al.*, Mapping region-specific longitudinal cortical surface expansion from birth to 2 years of age. *Cereb Cortex* **23**, 2724–2733 (2013).

24. G. Li, *et al.*, Mapping Longitudinal Development of Local Cortical Gyrification in Infants from Birth to 2 Years of Age. *J. Neurosci.* **34**, 4228–4238 (2014).
25. K. L. Bottenhorn, C. Cardenas-Iniguez, K. L. Mills, A. R. Laird, M. M. Herting, Profiling intra- and inter-individual differences in brain development across early adolescence. *NeuroImage* **279**, 120287 (2023).
26. K. L. Mills, *et al.*, Inter-individual variability in structural brain development from late childhood to young adulthood. *NeuroImage* **242**, 118450 (2021).
27. L. T. Strike, *et al.*, Genetic Complexity of Cortical Structure: Differences in Genetic and Environmental Factors Influencing Cortical Surface Area and Thickness. *Cereb Cortex* **29**, 952–962 (2019).
28. D. Alnæs, T. Kaufmann, A. F. Marquand, S. M. Smith, L. T. Westlye, Patterns of sociocognitive stratification and perinatal risk in the child brain. *Proc. Natl. Acad. Sci. U.S.A* **117**, 12419–12427 (2020).
29. A. L. Moreau, *et al.*, Prenatal Selective Serotonin Reuptake Inhibitor Exposure, Depression, and Brain Morphology in Middle Childhood: Results From the ABCD Study. *Biol Psychiatry Glob Open Sci* **3**, 243–254 (2022).
30. E. R. Sowell, *et al.*, Abnormal Cortical Thickness and Brain–Behavior Correlation Patterns in Individuals with Heavy Prenatal Alcohol Exposure. *Cereb Cortex* **18**, 136–144 (2008).
31. H. El Marroun, *et al.*, Prenatal Cannabis and Tobacco Exposure in Relation to Brain Morphology: A Prospective Neuroimaging Study in Young Children. *Biol Psychiatry* **79**, 971–979 (2016).
32. S. Treit, *et al.*, Longitudinal MRI reveals impaired cortical thinning in children and adolescents prenatally exposed to alcohol. *Hum Brain Mapp* **35**, 4892–4903 (2014).
33. M. L. Hartwell, J. M. Croff, A. S. Morris, F. J. Breslin, K. Dunn, Association of Prenatal Opioid Exposure With Precentral Gyrus Volume in Children. *JAMA Pediatr.* **174**, 893–896 (2020).
34. E. R. Sowell, *et al.*, Regional brain shape abnormalities persist into adolescence after heavy prenatal alcohol exposure. *Cereb Cortex* **12**, 856–865 (2002).
35. K. F. Casey, *et al.*, Birth weight discordance, DNA methylation, and cortical morphology of adolescent monozygotic twins. *Hum Brain Mapp* **38**, 2037–2050 (2017).
36. H. El Marroun, *et al.*, Association of Gestational Age at Birth With Brain Morphometry. *JAMA Pediatr.* **174**, 1149–1158 (2020).
37. M. Martinussen, *et al.*, Cerebral cortex thickness in 15-year-old adolescents with low birth weight measured by an automated MRI-based method. *Brain* **128**, 2588–2596 (2005).
38. K. B. Walhovd, *et al.*, Fetal influence on the human brain through the lifespan. *Elife* **12**, RP86812 (2024).
39. C. E. Kelly, *et al.*, Cortical growth from infancy to adolescence in preterm and term-born children. *Brain* **147**, 1526–1538 (2024).
40. Q. Zhou, *et al.*, Association of birth weight with neuropsychological functioning in early adolescence: A retrospective cohort study. *Psychiatry Research* **342**, 116183 (2024).
41. L. A. Wortinger, *et al.*, Asphyxia at birth affects brain structure in patients on the schizophrenia-bipolar disorder spectrum and healthy participants. *Psychological Medicine* **52**, 1050–1059 (2020).
42. NIMH Data Archive, ABCD Developmental History Questionnaire. *The National Institute of Mental Health Data Archive (NDA)* (2024). Available at: https://nda.nih.gov/data_structure.html?short_name=dhx01 [Accessed 25 March 2024].
43. E. A. Figueiró-Filho, *et al.*, Diffusion Tensor Imaging of White Matter in Children Born from Preeclamptic Gestations. *AJNR Am J Neuroradiol* **38**, 801–806 (2017).
44. M. T. Rätsep, *et al.*, Brain Structural and Vascular Anatomy Is Altered in Offspring of Pre-Eclamptic Pregnancies: A Pilot Study. *AJNR Am J Neuroradiol* **37**, 939–945 (2016).
45. K. M. Lynch, *et al.*, Selective morphological and volumetric alterations in the hippocampus of children exposed in utero to gestational diabetes mellitus. *Hum Brain Mapp* **42**, 2583–2592 (2021).

46. D.-S. Xuan, *et al.*, Brain Development in Infants of Mothers With Gestational Diabetes Mellitus: A Diffusion Tensor Imaging Study. *JCAT* **44**, 947 (2020).
47. C. A. Michalski, *et al.*, Association between maternal cannabis use and birth outcomes: an observational study. *BMC Pregnancy Childbirth* **20**, 771 (2020).
48. A. Umer, *et al.*, Prevalence of alcohol use in late pregnancy. *Pediatr Res* **88**, 312–319 (2020).
49. C. Nolte, K. J. Michalska, P. M. Nelson, Ö. E. Demir-Lira, Interactive roles of preterm-birth and socioeconomic status in cortical thickness of language-related brain structures: Findings from the Adolescent Brain Cognitive Development (ABCD) study. *Cortex* **180**, 1–17 (2024).
50. E. P. Davis, C. A. Sandman, C. Buss, D. A. Wing, K. Head, Fetal glucocorticoid exposure is associated with preadolescent brain development. *Biol Psychiatry* **74**, 647–655 (2013).
51. N. Khalife, *et al.*, Prenatal Glucocorticoid Treatment and Later Mental Health in Children and Adolescents. *PLOS ONE* **8**, e81394 (2013).
52. F. P. McCarthy, *et al.*, A Prospective Cohort Study Investigating Associations between Hyperemesis Gravidarum and Cognitive, Behavioural and Emotional Well-Being in Pregnancy. *PLoS One* **6**, e27678 (2011).
53. J. S. Seng, *et al.*, Posttraumatic Stress Disorder and Pregnancy Complications. *Obstet Gynecol* **97**, 17–22 (2001).
54. P. D. Wadhwa, *et al.*, Stress, infection and preterm birth: a biobehavioural perspective. *Paediatric and Perinatal Epidemiology* **15**, 17–29 (2001).
55. N. Dole, *et al.*, Maternal Stress and Preterm Birth. *American Journal of Epidemiology* **157**, 14–24 (2003).
56. C. Lebel, *et al.*, Prepartum and Postpartum Maternal Depressive Symptoms Are Related to Children's Brain Structure in Preschool. *Biological Psychiatry* **80**, 859–868 (2016).
57. E. P. Davis, *et al.*, Prenatal Maternal Stress, Child Cortical Thickness, and Adolescent Depressive Symptoms. *Child Development* **91**, e432–e450 (2020).
58. F. Rakers, *et al.*, Transfer of maternal psychosocial stress to the fetus. *Neurosci Biobehav Rev* **117**, 185–197 (2020).
59. J. R. Seckl, M. C. Holmes, Mechanisms of Disease: glucocorticoids, their placental metabolism and fetal "programming" of adult pathophysiology. *Nat Rev Endocrinol* **3**, 479–488 (2007).
60. K. O'Donnell, T. G. O'Connor, V. Glover, Prenatal Stress and Neurodevelopment of the Child: Focus on the HPA Axis and Role of the Placenta. *Developmental Neuroscience* **31**, 285–292 (2009).
61. J. Dy, H. Guan, R. Sampath-Kumar, B. S. Richardson, K. Yang, Placental 11β-Hydroxysteroid Dehydrogenase Type 2 is Reduced in Pregnancies Complicated with Idiopathic Intrauterine Growth Restriction: Evidence That This is Associated With an

Attenuated Ratio of Cortisone to Cortisol in the Umbilical Artery. *Placenta* **29**, 193–200 (2008).
62. C. O. McCalla, V. L. Nacharaju, O. Muneyyirci-Delale, S. Glasgow, J. G. Feldman, Placental 11 beta-hydroxysteroid dehydrogenase activity in normotensive and pre-eclamptic pregnancies. *Steroids* **63**, 511–515 (1998).
63. N. N. Nalivaeva, A. J. Turner, I. A. Zhuravin, Role of Prenatal Hypoxia in Brain Development, Cognitive Functions, and Neurodegeneration. *Front Neurosci* **12**, 825 (2018).
64. J. J. Volpe, Neonatal encephalopathy: An inadequate term for hypoxic–ischemic encephalopathy. *Ann Neurol* **72**, 156–166 (2012).
65. W. B. Stewart, L. R. Ment, M. Schwartz, Chronic postnatal hypoxia increases the numbers of cortical neurons. *Brain Res* **760**, 17–21 (1997).
66. M. Putra, E. Peek, J. C. Hobbins, Fetal insular measurements in pregnancy with estimated fetal weight <10th centile and childhood neurodevelopmental outcomes. *Am J Obstet Gynecol* **230**, 85.e1-85.e15 (2024).
67. G. Zhang, *et al.*, Genetic Associations with Gestational Duration and Spontaneous Preterm Birth. *N Engl J Med* **377**, 1156–1167 (2017).
68. L. Vasung, *et al.*, Association between Quantitative MR Markers of Cortical Evolving Organization and Gene Expression during Human Prenatal Brain Development. *Cereb Cortex* **31**, 3610–3621 (2021).
69. T. F. McNeil, E. Cantor-Graae, K. Sjöström, Obstetric complications as antecedents of schizophrenia: empirical effects of using different obstetric complication scales. *J Psychiatr Res* **28**, 519–530 (1994).
70. Q. A. Class, P. Lichtenstein, N. Långström, B. M. D'Onofrio, Timing of prenatal maternal exposure to severe life events and adverse pregnancy outcomes: a population study of 2.6 million pregnancies. *Psychosom Med* **73**, 234–241 (2011).
71. H. Garavan, *et al.*, Recruiting the ABCD sample: Design considerations and procedures. *Dev Cogn Neurosci* **32**, 16–22 (2018).
72. W. M. Compton, G. J. Dowling, H. Garavan, Ensuring the Best Use of Data. *JAMA Pediatr* **173**, 809–810 (2019).
73. L. B. Norbom, *et al.*, Parental education and income are linked to offspring cortical brain structure and psychopathology at 9–11 years. *JCPP Adv* **4**, e12220 (2024).
74. B. J. Casey, *et al.*, The Adolescent Brain Cognitive Development (ABCD) study: Imaging acquisition across 21 sites. *Dev Cogn Neurosci* **32**, 43–54 (2018).
75. D. J. Hagler, *et al.*, Image processing and analysis methods for the Adolescent Brain Cognitive Development Study. *NeuroImage* **202**, 116091 (2019).
76. B. Fischl, M. I. Sereno, A. M. Dale, Cortical Surface-Based Analysis: II: Inflation, Flattening, and a Surface-Based Coordinate System. *NeuroImage* **9**, 195–207 (1999).
77. A. M. Dale, B. Fischl, M. I. Sereno, Cortical Surface-Based Analysis: I. Segmentation and Surface Reconstruction. *NeuroImage* **9**, 179–194 (1999).
78. A. F. G. Rosen, *et al.*, Quantitative assessment of structural image quality. *NeuroImage* **169**, 407–418 (2018).
79. J.-P. Fortin, *et al.*, Harmonization of cortical thickness measurements across scanners and sites. *Neuroimage* **167**, 104–120 (2018).
80. A. R. Groves, C. F. Beckmann, S. M. Smith, M. W. Woolrich, Linked independent component analysis for multimodal data fusion. *NeuroImage* **54**, 2198–2217 (2011).
81. A. R. Groves, *et al.*, Benefits of multi-modal fusion analysis on a large-scale dataset: Life-span patterns of inter-subject variability in cortical morphometry and white matter microstructure. *NeuroImage* **63**, 365–380 (2012).
82. A. M. Auchter, *et al.*, A description of the ABCD organizational structure and communication framework. *Dev Cogn Neurosci* **32**, 8–15 (2018).
83. D. B. Clark, *et al.*, Biomedical ethics and clinical oversight in multisite observational neuroimaging studies with children and adolescents: The ABCD experience. *Dev Cogn Neurosci* **32**, 143–154 (2018).

84. M. E. Charness, The adolescent brain cognitive development study external advisory board. *Dev Cogn Neurosci* **32**, 155–160 (2018).

Figures and Tables

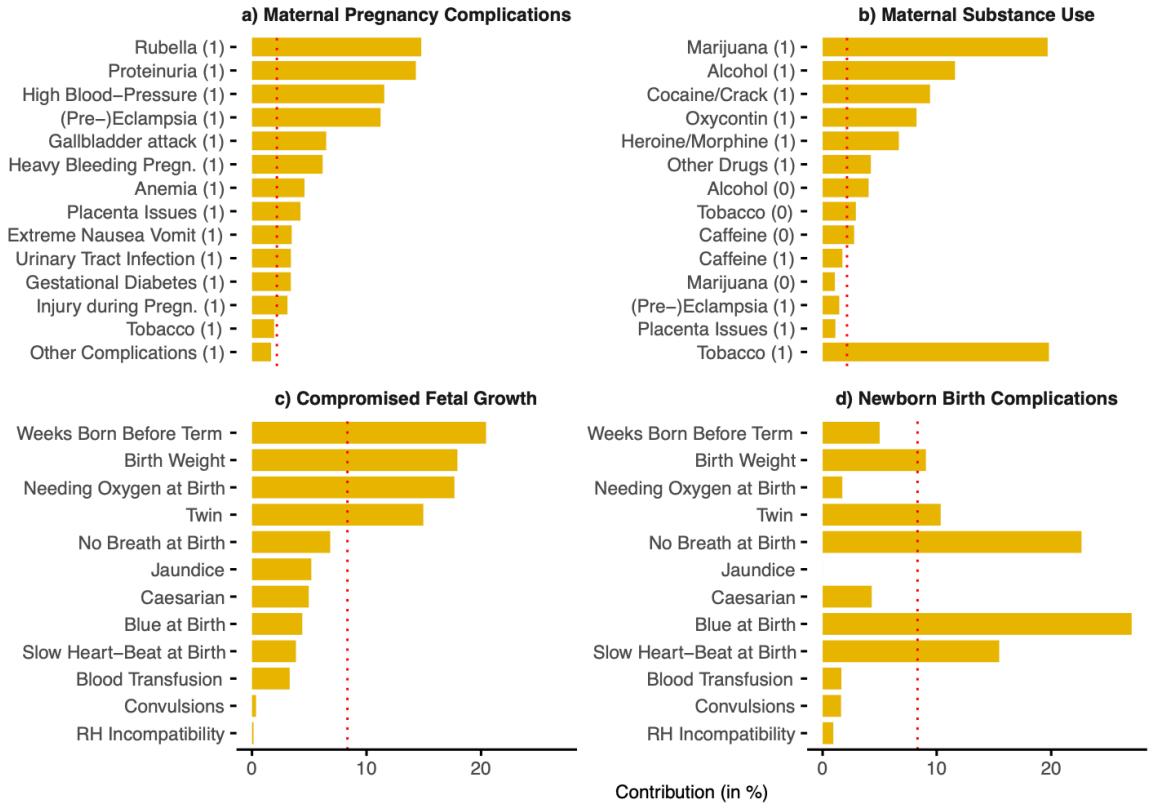

Figure 1. Variable contribution to pre- and perinatal dimensions. The figure shows the variables with the highest contributions to each dimension. The x-axis indicates the percentage contribution while the red dotted line represents the expected average contribution if the variables were uniform. a) and b) are prenatal dimensions while c) and d) are perinatal dimensions. (1) and (0) indicates whether the response to the variable is yes or no, respectively. Figure a) and b) show the top 14 contributing variables in the given dimension.

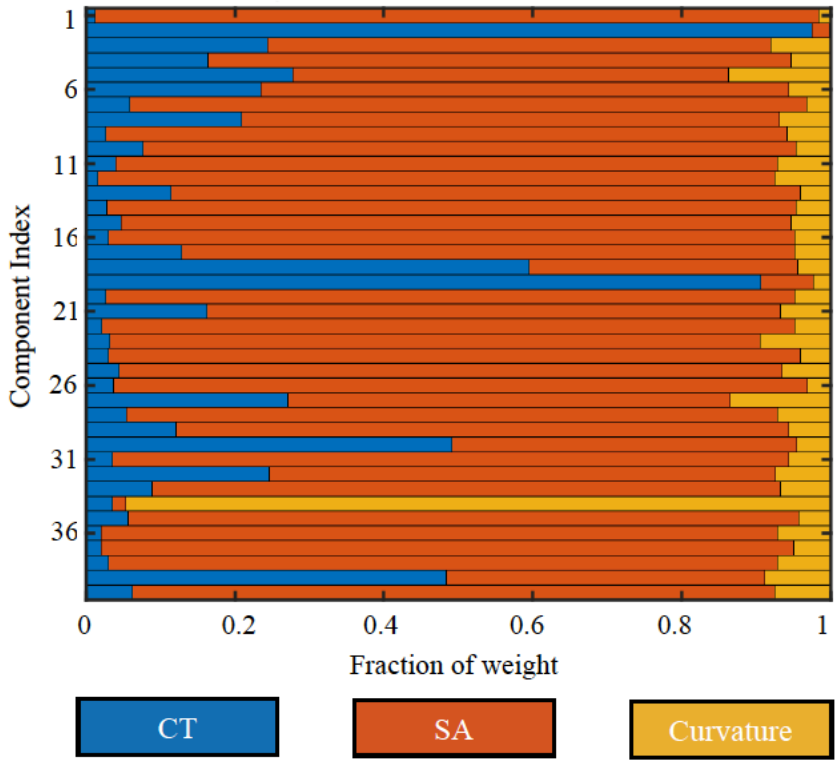

Figure 2. Cortical fusion decomposition. The figure shows the decomposition of the 40 cortical components, with relative weight of each of the three brain metrics CT (cortical thickness), SA (surface area), and Curvature.

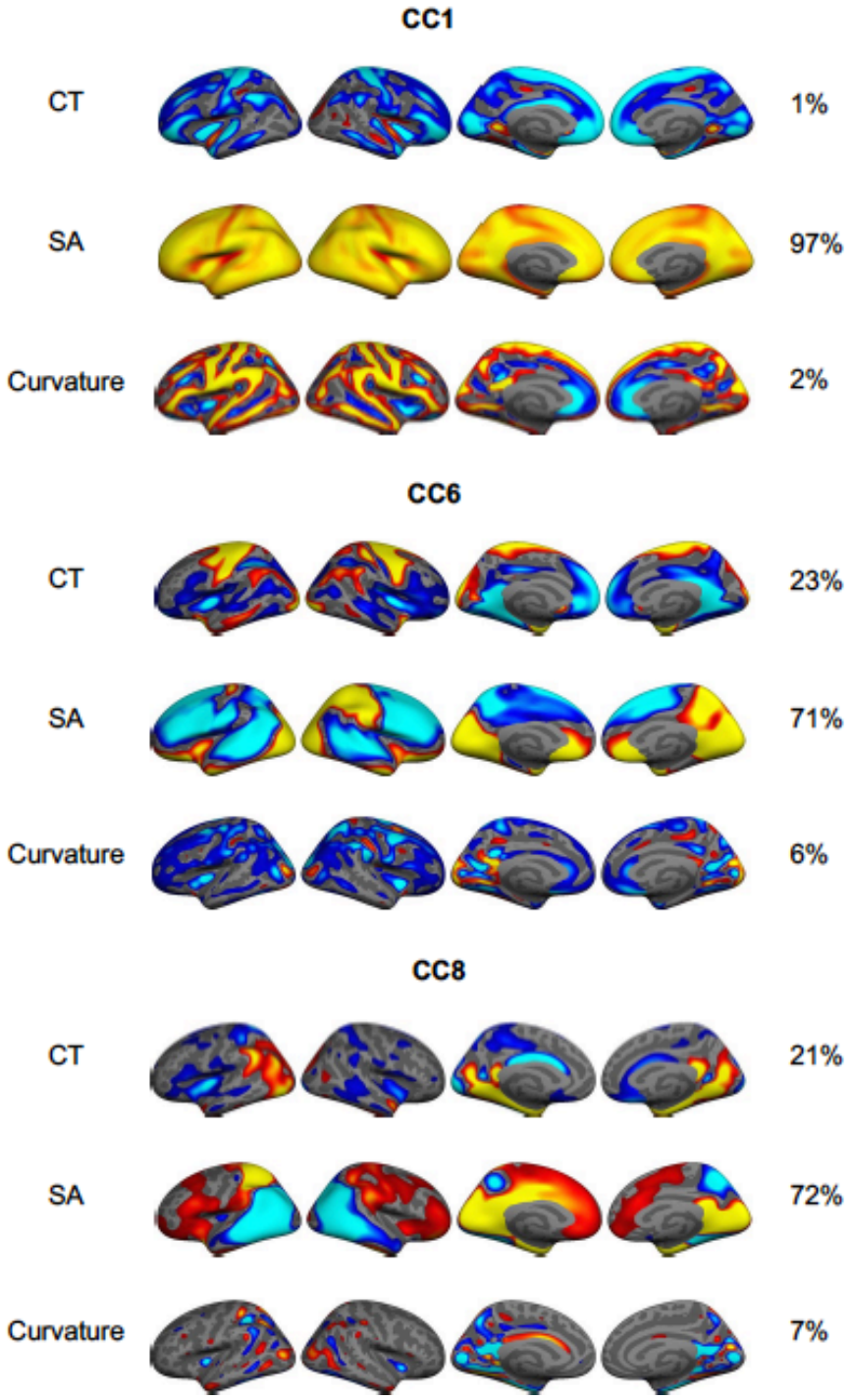

Figure 3. Cortical components associated with pre-and perinatal dimensions. The figure shows the cortical components (CC)s with a significant association with pre- and/or perinatal dimensions. All surface maps are thresholded with a minimum of 4 and maximum of 15 standard deviations, except for surface area within CC1, which were thresholded with a minimum of 20 and a maximum of 100, to enhance regional detail within the global pattern. Percentages represent the contributions of each metric within the CC.

Table 1. Associations between prenatal dimensions and CCs.

CC	Maternal Pregnancy Complications				Maternal Substance Use			
	Cohen´s D	t-value	p-value (unadj.)	p-value (adj.)	Cohen´s D	t-value	p-value (unadj.)	p-value (adj.)
1	-0.10	-4.50	**<0.001**	**<0.001**	0.02	0.67	0.504	0.985
2	-0.05	-2.32	**0.020**	0.730	0.01	0.26	0.796	0.985
3	-0.04	-1.56	0.118	0.997	0.05	2.31	**0.021**	0.766
4	0.00	0.02	0.983	0.997	0.00	0.05	0.963	0.985
5	0.02	1.04	0.298	0.997	0.03	1.29	0.196	0.985
6	-0.04	-1.80	0.072	0.997	-0.01	-0.63	0.529	0.985
7	0.01	0.61	0.545	0.997	0.02	0.85	0.394	0.985
8	-0.01	-0.28	0.776	0.997	-0.03	-1.20	0.230	0.985
9	-0.03	-1.14	0.253	0.997	0.01	0.35	0.724	0.985
10	-0.05	-2.04	**0.041**	0.997	-0.01	-0.59	0.554	0.985
11	0.02	0.65	0.516	0.997	-0.01	-0.26	0.797	0.985
12	0.04	1.67	0.094	0.997	0.00	-0.02	0.985	0.985
13	-0.01	-0.63	0.531	0.997	0.04	1.93	0.054	0.985
14	-0.06	-2.65	**0.008**	0.304	-0.04	-1.66	0.097	0.985
15	0.00	0.15	0.877	0.997	-0.03	-1.25	0.210	0.985
16	0.00	-0.20	0.842	0.997	-0.04	-1.86	0.063	0.985
17	0.00	0.00	0.997	0.997	0.02	0.80	0.424	0.985
18	0.01	0.30	0.761	0.997	0.05	2.22	**0.026**	0.949
19	-0.03	-1.42	0.155	0.997	0.02	0.73	0.466	0.985
20	-0.01	-0.33	0.742	0.997	-0.05	-2.36	**0.018**	0.708
21	-0.01	-0.35	0.726	0.997	-0.03	-1.52	0.128	0.985
22	0.02	0.63	0.527	0.997	-0.03	-1.47	0.140	0.985
23	0.00	-0.15	0.884	0.997	-0.02	-0.83	0.406	0.985
24	0.01	0.42	0.677	0.997	0.00	0.14	0.891	0.985
25	-0.04	-1.51	0.130	0.997	-0.01	-0.63	0.526	0.985
26	-0.02	-0.74	0.461	0.997	-0.05	-2.10	**0.036**	0.985
27	0.02	0.76	0.449	0.997	-0.02	-0.74	0.457	0.985
28	0.04	1.50	0.133	0.997	0.03	1.11	0.266	0.985
29	0.00	-0.19	0.853	0.997	0.03	1.44	0.150	0.985
30	-0.06	-2.59	**0.010**	0.358	0.03	1.27	0.203	0.985

31	0.02	0.86	0.392	0.997	0.01	0.36	0.717	0.985
32	-0.02	-0.84	0.399	0.997	0.01	0.36	0.717	0.985
33	0.01	0.59	0.556	0.997	0.05	2.33	**0.020**	0.763
35	0.00	-0.11	0.910	0.997	-0.02	-0.96	0.336	0.985
36	0.00	0.18	0.857	0.997	-0.01	-0.42	0.676	0.985
37	-0.01	-0.27	0.787	0.997	-0.03	-1.24	0.215	0.985
38	0.02	0.81	0.416	0.997	0.05	2.04	**0.042**	0.985
39	-0.03	-1.11	0.265	0.997	0.01	0.23	0.816	0.985
40	0.03	1.40	0.160	0.997	0.00	0.18	0.856	0.985

The table shows effect sizes, t-values, and uncorrected (Unadj.) and corrected (Adj.) p-values from the statistical analyses of the association between prenatal dimensions and cortical components (CC)s. Significant p-values are shown in bold.

Table 2. Associations between perinatal dimensions and CC.

CC	Compromised Fetal Growth				Newborn Birth Complications			
	Cohen´s D	t-value	p-value (unadj.)	p-value (adj.)	Cohen´s D	t-value	p-value (unadj.)	p-value (adj.)
1	-0.09	-3.93	**<0.001**	**0.003**	0.05	2.07	**0.038**	0.978
2	-0.01	-0.56	0.574	0.987	-0.03	-1.48	0.138	0.978
3	0.03	1.02	0.306	0.987	0.00	-0.22	0.828	0.978
4	-0.03	-1.15	0.249	0.987	0.01	0.45	0.656	0.978
5	0.06	2.28	**0.022**	0.675	-0.04	-1.75	0.080	0.978
6	-0.08	-3.24	**0.001**	**0.044**	0.01	0.61	0.545	0.978
7	-0.04	-1.39	0.165	0.987	0.06	2.90	**0.004**	0.144
8	0.10	4.15	**<0.001**	**0.001**	-0.06	-2.76	**0.006**	0.218
9	0.02	0.79	0.428	0.987	0.02	0.71	0.481	0.978
10	0.00	0.04	0.967	0.987	-0.02	-0.74	0.461	0.978
11	-0.03	-1.12	0.263	0.987	-0.02	-1.08	0.280	0.978
12	0.01	0.27	0.788	0.987	0.01	0.49	0.622	0.978
13	-0.01	-0.42	0.673	0.987	0.02	0.77	0.440	0.978
14	-0.06	-2.29	**0.022**	0.675	-0.03	-1.55	0.120	0.978
15	0.02	0.63	0.530	0.987	-0.02	-0.99	0.323	0.978
16	0.06	2.32	**0.020**	0.646	-0.04	-1.89	0.059	0.978
17	-0.05	-1.94	0.053	0.987	0.01	0.51	0.613	0.978
18	0.04	1.67	0.094	0.987	-0.01	-0.28	0.781	0.978
19	0.05	1.88	0.060	0.987	-0.01	-0.66	0.507	0.978
20	0.02	0.68	0.498	0.987	-0.04	-1.77	0.078	0.978
21	0.01	0.41	0.681	0.987	0.00	0.03	0.978	0.978
22	0.04	1.41	0.159	0.987	-0.01	-0.32	0.747	0.978
23	0.00	-0.02	0.987	0.987	0.01	0.49	0.624	0.978
24	-0.03	-0.96	0.336	0.987	0.00	-0.10	0.918	0.978
25	-0.04	-1.48	0.138	0.987	0.05	2.48	**0.013**	0.474
26	0.00	0.16	0.869	0.987	0.04	1.64	0.100	0.978
27	0.05	2.11	**0.035**	0.987	-0.03	-1.57	0.116	0.978
28	0.07	2.68	**0.007**	0.252	-0.04	-1.72	0.085	0.978
29	0.03	1.09	0.276	0.987	-0.02	-1.12	0.264	0.978
30	-0.01	-0.24	0.810	0.987	0.06	2.74	**0.006**	0.230
31	-0.07	-2.87	**0.004**	0.150	0.03	1.47	0.142	0.978

32	-0.07	-2.70	**0.007**	0.246	0.04	1.91	0.056	0.978
33	-0.03	-1.37	0.171	0.987	-0.01	-0.49	0.623	0.978
35	-0.01	-0.43	0.670	0.987	0.00	-0.08	0.937	0.978
36	0.01	0.26	0.795	0.987	-0.03	-1.17	0.244	0.978
37	0.01	0.49	0.626	0.987	-0.01	-0.45	0.655	0.978
38	0.03	0.92	0.356	0.987	-0.03	-1.53	0.125	0.978
39	0.06	2.52	**0.012**	0.383	-0.01	-0.68	0.495	0.978
40	0.03	1.00	0.316	0.987	-0.03	-1.14	0.255	0.978

The table shows effect sizes, t-values, and uncorrected (Unadj.) and corrected (Adj.) p-values from the statistical analyses of the association between prenatal dimensions and cortical components (CC)s. Significant p-values are shown in bold.